Heat transfer and flow characteristics of Al_2O_3/water nanofluid in various heat exchangers: Experiments on counter flow

Dariush Mansoury[1], Faramarz Ilami Doshmanziari[2], Abolfazl Kiani[3], Ali J. Chamkha[4,5], Mohsen Sharifpur[6]

[1]College of Marine Science, Tarbiat Modares University, Nour, Iran
[2]Department of Mechanical Engineering, Sahand University of Technology, Tabriz, Iran
[3]Engineering and Business Development Department, Jam Polypropylene Company, Tehran, Iran
[4]Mechanical Engineering Department, Prince Sultan Endowment for Energy and Environment, Prince Mohammad Bin Fahd University, Al-Khobar 31952, Saudi Arabia
[5]RAK Research and Innovation Center, American University of Ras Al Khaimah, P.O. Box 10021, Ras Al Khaimah, United Arab Emirates
[6]Department of Mechanical and Aeronautical Engineering, University of Pretoria, Pretoria, South Africa

Corresponding author;
Dariush Mansoury
Ph.D. in Physical Oceanography
Assistant Professor
Head of Department of Marine Physics
College of Marine Sciences, Tarbiat Modares University, Noor, Iran
46417-76489, Imam Reza Blvd. Noor, Mazandaran Province, Iran
Mansoury@modares.ac.ir
Tel.: (+98) 11 44553101; Mob.: (+98) 911 325 1537; Fax: (+98)11 44553499

Abstract

On account of nanofluids influence on heat exchangers, a vigorous discussion can be made to concurrently contrast heat exchangers to one another under the same conditions to detect maximum efficacy. Based on an extensive experimental study, this research is established to examine the effect of nanofluids on the performance of heterogeneous heat exchangers with the same heat transfer surface area considering counter flow arrangement. A double pipe heat exchanger, a shell & tube heat exchanger and a plate heat exchanger are intended to accomplish the experiments. The experiments are executed under turbulent flow conditions using distilled water and Al_2O_3/water nanofluid with 0.2%, 0.5%, and 1% particle volume concentrations. From

the results shown in the paper, the double pipe heat exchanger revealed the best outcome for the heat transfer coefficient with a maximum enhancement of 60% while a maximum enhancement in the heat transfer coefficient of 11% was reported for the plate heat exchanger. Utilizing a nanofluid represented the lowest penalty in the pressure drop with a maximum enhancement of 27% for the plate heat exchanger while the highest penalty in the pressure drop with a maximum enhancement of 85% was observed in the double pipe and shell & tube heat exchangers.

Introduction

Heat exchangers (HEs) are instruments that convey thermal energy between two or more fluids. HEs are applied in a vast variety of usages such as manufacturing industry, environmental engineering, air-conditioning, refrigeration, power production and space applications [1]. HEs are typically categorized according to flow arrangement and type of structure. Three major classifications of these devices are double pipe, shell & tube and plate (compact) HE. The arrangements for flow routes within a HE are parallel flow and counter one. In the parallel flow HE both working fluids in the HE flow in the same direction. In another arrangement the fluids flow in the opposite directions. Improvement of the HEs performance to attain higher productivity has been examined in the numerous studies. There are some techniques to increase heat transfer rate which are classified into two general categories: passive and active techniques [2, 3]. Generally, the conventional heat transfer fluids play a disagreeable role in heat transfer operation caused by their deficient thermal properties. Considering heat transfer enhancement techniques [2, 3] and based on the higher thermal conductivity of solids than liquids, additives such as solid particles can amend the thermal properties of the heat transfer fluids and therefore it would augment the efficiency of heat transfer surfaces. The early studies on suspensions containing millimeter- and micrometer-sized particles were encountered the problem of poor suspension

stability due to the large size and high density of the particles. Addition of nanoscale solid particles to the conventional heat transfer fluids, to fortify thermal properties and stability of suspension, was proposed by Choi and Eastman [4] in 1995. In the recent years, a large quantity of research attention has been allocated to the extension of nanofluids for the engineering applications of heat transfer. Das et al. [5] reported an extensive review of increment of heat transfer with nanofluids. Wen and Ding [6] studied experimentally convective heat transfer of γ-Al_2O_3/water nanofluid in a copper tube with a constant heat flux under laminar flow conditions. Williams et al. [7] investigated the effect of Alumina/Water and Zirconia/Water nanofluids on turbulent convective heat transfer and pressure loss in horizontal tubes experimentally. Heat transfer characteristics of Al_2O_3/water and Cu/water nanofluids in U-shaped enclosures at various Rayleigh numbers were numerically evaluated by Snoussi et al. [8]. Considering counter flow arrangement, heat transfer and flow characteristics of TiO_2/water nanofluid in a horizontal double tube HE were experimentally studied by Duangthongsuk and Wongwises [9]. Pantzali et al. [10] studied performance of nanofluid as a coolant in a typical commercial herringbone-type plate heat exchanger (PHE) experimentally. Mare et al. [11] carried out some experiments to investigate thermal performances of Al_2O_3/water and aqueous suspensions of nanotubes of carbons (CNTs) nanofluids in a PHE. Effects of Al_2O_3/water nanofluid on heat transfer, frictional losses and exergy loss in a counter flow corrugated PHE were experimentally investigated by Pandey and Nema [12]. Tiwari et al. [13] investigated the effects of various nanofluids (CeO_2, Al_2O_3, TiO_2 and SiO_2) on performance of a PHE experimentally. Reddy and Rao [14] studied experimental characteristics of heat transfer and flow of ethylene glycol water-based TiO_2 nanofluid in a double pipe heat exchanger with and without helical coil inserts. Based on an experimental study, Tshimanga et al. [15] developed a model for thermal conductivity of Glycerol-MgO nanofluids at different volume fractions and

sizes. Considering experimental and numerical studies, Doshmanziari et al. [16] examined the heat transfer and flow characteristics of Al_2O_3/water nanofluid in a spiral-coil tube under turbulent flow regime.

From the nanofluid effect point of view on HEs, it will be exquisite to simultaneously compare HEs to one another under the same conditions to discover the maximum effectiveness. Although some papers are presently attainable on the investigation of convective heat transfer of nanofluids in different HEs, however, the present investigation plans to concentrate on an extensive study of the influence of Al_2O_3/water nanofluid on the performance of different HEs with the counter-flow arrangement to find out an appropriate HE under the same experimental conditions. In fact, in the open literature, there is no reported research to reflect the comparison of the traditional HEs performance using nanofluids at the same condition. The present paper will cover and complete all current studies related to these issues.

Details of experimental apparatus and procedure

Preparation and properties of nanofluid

In this study, alumina nanoparticles with average diameter of 20 nm are used which are produced by US Research Nanomaterials, Inc. **Fig. 1** depicts SEM and TEM images provided by the manufacturer and verifies the nanoparticles size and shape mentioned in the nanoparticles specification. It can be observed from the images that the nanoparticles have reasonable size and shape corresponding to the nanoparticles specification provided by the manufacturer. Furthermore, the images depict appropriate size distribution of the alumina nanoparticles. The particle size is one of the important parameters in predicting the thermal conductivity and viscosity of nanofluids, therefore, SEM and/or TEM are very important to calculate the heat transfer enhancements accuratly. The thermal conductivity, density and the specific heat capacity of Al_2O_3 nanoparticles

are 40 $W.m^{-1}.K^{-1}$, 3890 $kg.m^{-3}$ and 880 $J.kg^{-1}.K^{-1}$, respectively. The nanoparticles with volume concentrations of 0.2%, 0.5% and 1% are first stirred in deionized water and then sonicated by an ultrasonic homogenizer (UHP-400, manufactured by TOPSONICS) at 400W and 20 kHz for 1 h. No surfactant is exerted to stabilize the nanoparticles. After 24 h, pH values of the prepared nanofluids were between 5 and 6. The measured pH values were away from the isoelectric point of 9.2 for alumina nanoparticles. It showed that the dispersed nanoparticles were physically stable in the base fluid [17].

The density and heat capacity of the nanofluid are determined using the following relations [18]:

$$\rho_{nf} = \varphi\rho_p + (1-\varphi)\rho_{bf} \tag{1}$$

$$C_{p,nf} = \frac{\varphi(\rho C_p)_p + (1-\varphi)(\rho C_p)_{bf}}{\rho_{nf}} \tag{2}$$

where the subscripts *nf*, *p* and *bf* indicate nanofluid, nanoparticle and base fluid, respectively.

Corcione [19] proposed a correlation to estimate the effective thermal conductivity of the nanofluids as follows:

$$\frac{k_{nf}}{k_{bf}} = 1 + 4.4 Re_p^{0.4} Pr_{bf}^{0.66} \left(\frac{T}{T_{fr}}\right)^{10} \left(\frac{k_p}{k_{bf}}\right)^{0.03} \varphi^{0.66} \tag{3}$$

where T_{fr} is the freezing point of the base liquid and Re_p is the nanoparticle Reynolds number, calculated by the following equation:

$$Re_p = \frac{\rho_{bf} u_B d_p}{\mu_{bf}} = \frac{2\rho_{bf} K_B T}{\pi \mu_{bf}^2 d_p} \tag{4}$$

where K_B and d_p are the Boltzmann's constant 1.38066×10-23 $J.K^{-1}$ and the average diameter of nanoparticles, respectively.

To estimate the dynamic viscosity of nanofluids, the following equation is used [19]:

$$\frac{\mu_{nf}}{\mu_{bf}} = \frac{1}{1 - 34.87\left(\frac{d_p}{d_{bf}}\right)^{-0.3}\varphi^{1.03}} \tag{5}$$

where d_{bf} is the equivalent diameter of a molecule of the base fluid:

$$d_{bf} = \left(\frac{6M}{N\pi\rho_{f0}}\right)^{1/3} = \left(\frac{6\times 0.01801528}{6.022\times 10^{23}\times\pi\times 998.26}\right)^{1/3} = 3.85\times 10^{-10}\,\mathrm{m} \tag{6}$$

where M, N and ρ_{f0} are the molecular weight of the base fluid, Avogadro number and the mass density of the base fluid at temperature 293 K, respectively.

The used correlations for the nanofluid properties are obtained from an extensive range of experimental measurements related to the nanofluids including AL_2O_3, CuO and TiO_2 nanoparticles with water or ethylene glycol base fluids. The correlations for the thermal conductivity and the viscosity of the nanofluid, Eq. (3) and Eq. (5), are ranged from 10 nm to 200 nm for nanoparticles diameter, from 0.2% to 9% for volume concentration and from 293 K to 333 K for temperature, with 1.86% and 1.84% standard deviations, respectively.

Experimental setup

An experimental test rig setup is designed and constructed to investigate the effect of the nanofluid on the performance of various HEs as shown in **Fig. 2**. The experimental setup mainly comprises of a stainless steel structure for installing equipment, fluid supply unit, data acquisition system and three HEs (with the same heat transfer surface area, 0.4 m^2). The fluid supply unit consists of storage tanks, pumps, flow route control valves and flowmeters. Three 3 kW electrical

heaters and one electrical heater of 4 kW are installed at the bottom of the storage tank of the hot fluid (nanofluid). A PT100 temperature sensor of 0.1 ^{0}C accuracy is submerged in the storage tank to measure the temperature of the nanofluid. A 12V agitator of 220 rpm is located in the storage tank to put the nanofluid into motion by rotating. The nanofluid is pumped out of the storage tank by stainless steel centrifugal pump (LEO, Model AMS210/1.1) while cold water (cold fluid) is poured into the HEs by stainless steel centrifugal pump (CNP, Model MS60/0.75). The nanofluid flow route is automatically specified via the ¾ inch stainless steel solenoid valves and the control unit to test an intended HE. A calibrated turbine flowmeter (Model, LWGY) with an accuracy of ±1% is used to measure the volumetric flow rate of the nanofluid. To estimate the volumetric flow rate of the cold water, a calibrated flowmeter (ZENNER, MTKD-N) is also installed on the way of the flow. Three types of HEs including the double pipe, shell & tube and plate HEs are designed and constructed to fulfill the experiments.

The structure of the double pipe HE (hairpin HE) is shown in **Fig. 3(a)**. The double pipe HE is comprised of two concentric stainless steel tubes. The inner pipe has a 3220 mm length, an outer diameter of 42.2 mm and 2.77 mm thickness, while the annulus has an outer diameter of 63 mm and 1 mm thickness. The nanofluid as the hot fluid is passed through the inner pipe while cold water is flowing through the annulus. Ten calibrated K type thermocouples of 0.5 ^{0}C accuracy are mounted at different positions on the outer surface of the HE to measure local temperatures of the outer surface of the annulus.

As shown in **Fig. 3(b)**, the shell & tube HE (one shell pass and one tube pass) consists of a stainless steel shell with an outer diameter of 114.3 mm and 3 mm thickness and fifteen stainless steel tubes with length of 1000 mm and inner and outer diameters of 7.3 mm and 9.5 mm, respectively. Pitch of the tubes and baffle cut are 18 mm and 25%, respectively. The nanofluid as

the hot fluid is flowing inside the tubes while the cold water is entered inside the shell. To measure local temperatures of the outer surface of the shell, five calibrated K type thermocouples are installed along the outer surface of the shell at equal spaces.

A PHE consists of 30 stainless steel corrugated plates that generate two isolated fluid routes for the nanofluid (hot fluid) flow and cold water one respectively, considering fifteen flow channels per stream. Each channel has a 193 mm length (A') and an 83 mm width (C'). The plates have chevron-type corrugations with a depth (b) of 1.9 mm and chevron angle (β) of 45^{o} relative to the direction of the flow. The port diameter (D_{port}) and the thickness (t) of the plate are 19 mm and 0.4 mm, respectively. The vertical and horizontal distances (B', D') between the ports are 154 mm and 42 mm, respectively. Schematic depiction of a corrugated plate of the PHE is presented in **Fig. 3(c)**.

For each HE, four calibrated PT100 temperature sensors of 0.1 ^{0}C accuracy are directly placed into the fluid flow at the inlet and outlet of the HE to measure bulk temperatures of the working fluids. To determine pressure drop along the test section of the HEs, a differential pressure transmitter (Rosemount 3051CD) with an accuracy of ±0.05% is installed on the test rig setup. The HEs are thermally isolated to minimize heat loss through their walls and reduce heat loss along the axial direction.

Experimental procedure

Heat transfer and flow characteristics of Al_2O_3/water nanofluid in three counter flow HEs are evaluated using the following experimental procedure. Based on the experimental program, the nanofluid suspension is sonicated and then the pH value of the nanofluid is measured to ensure the stability of the nanofluid. In the experiments, the nanofluid is utilized as the hot fluid while water flows as the coolant. In order to heat the nanofluid inside the reservoir tank, the electrical

heaters are switched on, and the initial temperature of the nanofluid is controlled and maintained at 45 ^{0}C during the experimental process. All experiments on the nanofluid are performed under turbulent flow conditions. Inlet temperature and flow rate of the cold water are constant during the experiments to create the same conditions for all these HEs. For all volume concentrations of the nanoparticles and different flow rates, inlet and outlet temperatures of HEs are recorded, after achieving the steady-state condition. To record the experimental data, each experiment takes 20–30 minutes to get the steady-state. During this time period of the steady-state, the temperatures were recorded every couple of seconds for adequate numbers, and the average between the accumulated values is considered as the final result. A LabVIEW system engineering software is employed to control the experimental setup. Finally, the results are depicted in the monitor as shown in **Fig. 4** and are recorded in excel files.

Uncertainty analysis

An uncertainty analysis for the experiments is performed by Kline and McClintock method [20]. The dependent variable, R, is defined as a function of the independent variables V_i, $1 \le i \le n$, where n is the number of independent variables. U_R and U_{Vi} are the uncertainties for the results and the independent variables, respectively. The results of the uncertainty analysis are shown in **Table 1**.

$$U_R = \left[\sum_{i=1}^{n} \left(\frac{\partial R}{\partial V_i} U_{V_i} \right)^2 \right]^{\frac{1}{2}} \tag{7}$$

Data reduction

For the double pipe HE, heat transfer rate from the hot fluid, Q_h, is defined as shown [21]:

$$Q_h = \dot{m}_h C_{ph} (T_{hi} - T_{ho}) \tag{8}$$

where $\dot{m}_h$ is mass flow rate of the hot fluid, C_{ph} is the specific heat of the hot fluid, T_{hi} and T_{ho} are inlet and outlet bulk temperatures of the hot fluid, respectively.

The heat transfer rate absorbed by the cold water, Q_c, is calculated by:

$$Q_c = \dot{m}_c C_{pc} (T_{co} - T_{ci}) \tag{9}$$

where $\dot{m}_c$ is mass flow rate of the cold fluid, C_{pc} is specific heat of the cold fluid, T_{ci} and T_{co} are inlet and outlet bulk temperatures of the cold fluid, respectively.

The overall heat transfer coefficient, U_o, is defined as shown [21]:

$$U_o = \frac{Q_{ave}}{A_o \Delta T_{lm}} = \frac{1}{\frac{A_o}{A_i h_i} + \frac{A_o \ln(D_o / D_i)}{2\pi L k_{ss}} + \frac{1}{h_o}} \tag{10}$$

where Q_{ave} is average value of the heat transfer rates, A_o and A_i are outside and inside heat transfer surface areas of the inner pipe, D_o and D_i are outside and inside diameters of the inner pipe, k_{ss} is the thermal conductivity of the inner pipe, L is the inner pipe length, h_i and h_o are heat transfer coefficients of the hot and cold fluids and ΔT_{lm} is counter flow logarithmic mean temperature difference, which is obtained from [21]:

$$\Delta T_{lm,counterflow} = \frac{(T_{hi} - T_{co}) - (T_{ho} - T_{ci})}{\ln \frac{(T_{hi} - T_{co})}{(T_{ho} - T_{ci})}} \tag{11}$$

The annulus side heat transfer coefficient is determined using:

$$h_o = \frac{Q_c}{(\pi D_H L)(T_s - T_{mc})} \tag{12}$$

where T_{mc} is the mean bulk temperature of the cold water, T_s is the average temperature of the annulus wall surface, and D_H is the annulus hydraulic diameter which are obtained by:

$$T_s = \frac{\sum_{i=1}^{10} T_i}{10} \tag{13}$$

$$D_H = \frac{D_2^2 - D_1^2}{D_1} \tag{14}$$

where T_i is the local temperature of the annulus wall, D_2 and D_1 are the outside and the inside diameters of the annulus, respectively.

Finally, h_i is calculated using Eq. (10) and the Nusselt number of the hot fluid, Nu_i, is determined by:

$$Nu_i = \frac{h_i D_i}{k_{fh}} \tag{15}$$

where k_{fh} is the thermal conductivity of the hot fluid.

The Gnielinski correlation [22] for a single-phase flow is represented as follows:

$$Nu = \frac{(f/8)(Re - 1000)Pr}{1 + 12.7(f/8)^{1/2}(Pr^{2/3} - 1)} \qquad 0.5 \le Pr \le 2000, 3000 \le Re \le 5\text{x}10^6 \tag{16}$$

where Friction factor, f, is obtained from Blasius equation, $f = 0.079Re^{-0.25}$, 4000≤Re≤100000.

For the shell & tube HE, the heat transfer rates of the hot and cold fluids are calculated by using equations (8) and (9), respectively.

The overall heat transfer coefficient, U_i, is defined as [21]:

$$U_i = \frac{Q_{ave}}{A_i \Delta T_{lm}} = \frac{1}{\frac{1}{h_i} + \frac{A_i \ln(D_o / D_i)}{2\pi L k_{ss}} + \frac{A_i}{A_o h_o}} \tag{17}$$

The shell side heat transfer coefficient is determined using:

$$h_o = \frac{Q_c}{A(T_s - T_{mc})} \tag{18}$$

For the shell & tube HE, the heat transfer surface area, A, is 0.4 m^2. T_s is the average temperature of the shell wall that is obtained by:

$$T_s = \frac{\sum_{i=1}^{5} T_i}{5} \tag{19}$$

According to the previous methodology, the other parameters are calculated.

For the PHE, the heat transfer rates of the hot and cold fluids are calculated by using equations (8) and (9), respectively.

The conduit hydraulic diameter, D_H, superficial velocity inside the conduit, U_S, and the Reynolds number are obtained by [10]:

$$Re = \frac{\rho D_H U_S}{\mu} \tag{20}$$

$$D_H = 2b \tag{21}$$

$$U_S = \frac{V}{nbB} \tag{22}$$

where b is the corrugation depth, V is the volumetric flow rate, B is the plate width, and n is number of passes per stream.

The overall heat transfer coefficient, U, is calculated as [1]:

$$U = \frac{Q_{ave}}{A \Delta T_{lm}} = \frac{1}{\frac{1}{h_i} + \frac{t}{k_{ss}} + \frac{1}{h_o}} \tag{23}$$

where, t is the plate thickness. For the PHE, the heat transfer surface area, A, is 0.42 m^2.

The Nusselt number and the heat transfer coefficient of the cold water are calculated from the following correlation with 3.91% mean error [23]:

$$Nu_o = \frac{h_o D_H}{k_{fc}} = 0.2302 Re_c^{0.745} Pr_c^{0.4} \qquad 58 < Re < 624 \tag{24}$$

where K_{fc} is the thermal conductivity of the cold water. In the present study, the Reynolds number of the cold water is maintained at 600. Ultimately, h_i is determined using Eq. (23).

Vlasogiannis et al. [24] obtained the following correlation with a maximum spread of the data of 6% to calculate the Nusselt number in a PHE:

$$Nu = 0.51 Re^{0.58} Pr^{0.33} \qquad Re > 650 \tag{25}$$

For the PHE, the overall pressure drop measured by the differential pressure transmitter, ΔP, is defined as follows [1]:

$$\Delta P = \Delta P_{ch} + \Delta P_{port} \tag{26}$$

where ΔP_{ch} and ΔP_{port} are the pressure drops in the channels and the port, respectively.

The port pressure drop is calculated from [1]:

$$\Delta P_{port} = \frac{1.4 \rho V_{Port}^2}{2} \tag{27}$$

where, V_{port} is the mean velocity of the fluid at the port. Eventually, ΔP_{ch} is obtained from Eq. (26).

Results and discussion

Comparison of measurements

Fig. 5 depicts the variation of the Nusselt number versus the Reynolds number for de-ionized water flowing in the different HEs. For the double pipe HE, the experimental results have 91% agreement with the correlation reported by Gnielinski et al. [22], Eq. (16). For the shell &

tube HE, this figure illustrates a 92% consensus between the Nusselt numbers obtained from the present data with those extracted from the Gnielinski correlation [22], Eq. (16). The distinction in the test section geometry and the uncertainties of instruments are the reasons for the discrepancy between the present results and the mentioned correlation [22]. For the PHE, this figure also displays a comparison of the Nusselt numbers between the present data and those extracted from the available correlation [24], Eq. (25), to evaluate the reliability of the measurements. From the information presented in this figure, a 93% agreement between the measured results and the predicted values is obtained.

Heat transfer

The behavior of the average heat transfer rate with respect to the Reynolds number at different nanoparticle concentrations for the various HEs is revealed in **Fig. 6**. For the double pipe HE, at 0.2%, 0.5% and 1% volume concentrations of the nanofluid, the heat transfer rates of the nanofluid are increased compared with those of water up to 33%, 18% and 46%, respectively. Heat transfer augmentation by using nanofluids may be caused by the thermal conductivity enhancement, energy transfer by nanoparticles dispersion, Brownian motion of particles, particle migration, reduction of boundary layer thickness and delay in the boundary layer development [6, 18, 25]. As shown in this figure, for the shell & tube HE, at 0.2% volume concentration, there is a small increase in the heat transfer rates of the nanofluid with a maximum of 12%. For 0.5% and 1% volume concentrations of the nanofluid, the heat transfer rates of the nanofluid are ranged from 3% to 20% and 4% to 24%, respectively. According to the figure, the nanofluid has no significant effect on the performance of the PHE, especially at the high volume concentrations. Moreover, there is a gentle reduction in the heat transfer rates of the nanofluid with a maximum reduction of 3% at 1% volume concentration compared with those of water. According to Eq. (3), it is apparent

that increase in the nanoparticle concentration leads to an increase in the thermal conductivity. On the other hand, based on Eq. (5), the increase in nanoparticle concentration increases the fluid viscosity and therefore, a drop in the heat transfer rate. These results reveal that the negative effect of the viscosity enhancement can overcome the positive influence of the thermal conductivity increment under the conditions of this study. For the PHE and the nanofluid of 0.5% volume concentration, there is a small increase in the heat transfer rates with a maximum of 11%.

The behavior of the Nusselt number ratio with respect to the Reynolds number at the different nanoparticle concentrations for the various HEs is revealed in **Fig. 7**. For the double pipe HE, at a given nanoparticle concentration, the Nusselt number ratio increases with increasing the Reynolds number. The maximum enhancement in the Nusselt number of 60% is observed at 1% volume concentration. For the shell & tube HE, there is a moderate increase in the Nusselt number at the low and high Reynolds numbers while at the medium Reynolds numbers, a small increase in the Nusselt number can be seen. For the PHE, there is a minimal increase in the Nusselt number. Also, the Nusselt number ratio does not change with increasing values of the Reynolds number especially at the medium and high flow rates.

Pressure drop

Fig. 8 depicts the variation of the pressure drop along the test section of the HEs versus the Reynolds number for various volume concentrations of the nanofluid. It is observed that at a given Reynolds number, the pressure drop of the nanofluid increases through raising the nanoparticle concentration due to the increment in the fluid viscosity. For the double pipe HE, at 0.2%, 0.5% and 1% volume concentrations, the pressure drop increases from 8% to 33%, from 18% to 72% and from 27% to 83%, respectively. Similar results for the heat transfer and the pressure drop of the nanofluids in double pipe HEs are observed in the literature [9, 14, 26, 27]. For the shell &

tube HE, as shown in this figure, at 0.2%, 0.5% and 1% volume concentrations the pressure drop of the nanofluid is increased compared with that of water up to 25%, 75% and 85%, respectively. Some researchers [28-31] reported similar results for the heat transfer and the pressure drop in the shell and tube HEs. For the PHE, it can be observed that at 0.2%, 0.5% and 1% volume concentrations of the nanofluid, the maximum pressure drops are 19%, 23% and 27%, respectively. These trends of the nanofluids heat transfer and pressure drop in PHEs agree with the literature [10, 23, 32, 33].

Conclusion

This paper was conducted to investigate the effect of Al_2O_3/water nanofluid on the heat transfer and the pressure drop in sundry HEs with counter flow arrangement. With a maximum enhancement of 60% in the heat transfer coefficient originated in the nanofluid, the double pipe HE illustrated the best result while the PHE reflected 11% increment in the heat transfer coefficient. A slight decrease in the heat transfer coefficient was also observed for the PHE. From the obtained research data, it was concluded that the smallest percentage of the pressure drop due to the nanoparticles were reflected in the PHE compared with the results obtained for the other HEs. This article has only been able to touch on the most general features of Al_2O_3/water nanofluid on the heat transfer in the HEs. In order to acquire higher efficiency in the HEs, evaluation of other nanofluids will be helpful through further investigations.

Funding

The authors thank the Jam Polypropylene Company, Islamic Azad University of Nour Branch and the Iran Nanotechnology Initiative Council (INIC) for their financial support for this study.

Nomenclature

A heat transfer surface area, m^2

A' plate length, m

b corrugation depth, m

B' vertical distance between ports, m

C' plate width, m

C_p specific heat capacity, $J.kg^{-1}.K^{-1}$

d_{bf} equivalent diameter of a molecule of the base fluid, m

d_p average diameter of nanoparticles, nm

D diameter of tube, m

D' horizontal distance between ports, m

D_1 inside diameter of annulus, m

D_2 outside diameter of annulus, m

f Blasius friction factor

h convective heat transfer coefficient, $W.m^{-2}.K^{-1}$

HE Heat exchanger

k thermal conductivity, $W.m^{-1}.K^{-1}$

K_B Boltzmann's constant, $J.K^{-1}$

L length of tube, m

$\dot{m}$ mass flow rate, $kg.s^{-1}$

M molecular weight of the base fluid, $kg.kmol^{-1}$

n number of passes per stream

N Avogadro number

Nu Nusselt number

PHE Plate heat exchanger

Pr Prandtl number

Q heat transfer rate, W

Re Reynolds number

Re_p nanoparticle Reynolds number

SEM	Scanning Electron Microscope
t	plate thickness, m
T	temperature, K
T_i	local temperature of the wall surface, K
T_s	average temperature of the wall surface, K
T_0	temperature at the inlet, K
TEM	Transmission Electron Microscopy
u_B	Brownian velocity of the nanoparticle, $m.s^{-1}$
U	overall heat transfer coefficient, $W.m^{-2}.K^{-1}$
U_S	superficial velocity inside the conduit, $m.s^{-1}$
V	volume flow rate, $m^3.s^{-1}$

Greek symbols

β	chevron angle, ^{0}
μ	dynamic viscosity, $kg.m^{-1}.s^{-1}$
ρ	density, $kg.m^{-3}$
ρ_{f0}	mass density of the base fluid at temperature 293 K, $kg.m^{-3}$
φ	nanoparticle volumetric fraction
ΔP	pressure drop, kPa
ΔT_{lm}	logarithmic mean temperature difference, K

Subscripts

ave	average
bf	base fluid
c	cold
ch	channel
f	fluid
fr	freezing
h	*hot*

H *Hydraulic*

i inside

m mean

nf nanofluid

o outside

p nanoparticle

s wall surface

ss stainless steel

w water

References

[1] Kakac, S., Liu, H., and Pramuanjaroenkij, A., *Heat Exchangers: Selection, Rating, and Thermal Design*: CRC press, 2012.

[2] Bergles, A., "Some Perspectives on Enhanced Heat Transfer-Second-Generation Heat Transfer Technology," *Journal of Heat Transfer,* vol. 110, no. 4b, pp. 1082-1096, 1988.

[3] Bergles, A., Techniques to enhance heat transfer, in *Handbook of Heat Transfer,* vol. 3, pp. 11.1-11.76, 1998.

[4] Choi, S. U. S., and Eastman, J. A., Enhancing thermal conductivity of fluids with nanoparticles, Argonne National Lab., IL (United States)1995.

[5] Das, S. K., Choi, S. U. S., and Patel, H. E., "Heat transfer in nanofluids—a review," *Heat Transfer Engineering,* vol. 27, no. 10, pp. 3-19, 2006.

[6] Wen, D., and Ding, Y., "Experimental investigation into convective heat transfer of nanofluids at the entrance region under laminar flow conditions," *International Journal of Heat and Mass Transfer,* vol. 47, no. 24, pp. 5181-5188, 2004.

[7] Williams, W., Buongiorno, J., and Hu, L. W., "Experimental investigation of turbulent convective heat transfer and pressure loss of alumina/water and zirconia/water nanoparticle

colloids (nanofluids) in horizontal tubes," *Journal of Heat Transfer,* vol. 130, no. 4, p. 042412, 2008.

[8] Snoussi, L., Ouerfelli, N., Chesneau, X., Chamkha, A. J., Belgacem, F. B. M., and Guizani, A., "Natural Convection Heat Transfer in a Nanofluid Filled U-Shaped Enclosures: Numerical Investigations," *Heat Transfer Engineering,* pp. 1-11, 2017. Latest Articles

[9] Duangthongsuk, W., and Wongwises, S., "Heat transfer enhancement and pressure drop characteristics of TiO_2–water nanofluid in a double-tube counter flow heat exchanger," *International Journal of Heat and Mass Transfer,* vol. 52, no. 7-8, pp. 2059-2067, 2009.

[10] Pantzali, M., Mouza, A., and Paras, S., "Investigating the efficacy of nanofluids as coolants in plate heat exchangers (PHE)," *Chemical Engineering Science,* vol. 64, no. 14, pp. 3290-3300, 2009.

[11] Maré, T., Halelfadl, S., Sow, O., Estellé, P., Duret, S., and Bazantay, F., "Comparison of the thermal performances of two nanofluids at low temperature in a plate heat exchanger," *Experimental Thermal and Fluid Science,* vol. 35, no. 8, pp. 1535-1543, 2011.

[12] Pandey, S. D., and Nema, V., "Experimental analysis of heat transfer and friction factor of nanofluid as a coolant in a corrugated plate heat exchanger," *Experimental Thermal and Fluid Science,* vol. 38, pp. 248-256, 2012.

[13] Tiwari, A. K., Ghosh, P., and Sarkar, J., "Performance comparison of the plate heat exchanger using different nanofluids," *Experimental Thermal and Fluid Science,* vol. 49, pp. 141-151, 2013.

[14] Reddy, M. C. S., and Rao, V. V., "Experimental investigation of heat transfer coefficient and friction factor of ethylene glycol water based TiO_2 nanofluid in double pipe heat

exchanger with and without helical coil inserts," *International Communications in Heat and Mass Transfer,* vol. 50, pp. 68-76, 2014.

[15] Tshimanga, N., Sharifpur, M., and Meyer, J. P., "Experimental Investigation and Model Development for Thermal Conductivity of Glycerol–MgO Nanofluids," *Heat Transfer Engineering,* vol. 37, no. 18, pp. 1538-1553, 2016.

[16] Doshmanziari, F. I., Kadivar, M. R., Yaghoubi, M., Jalali-Vahid, D., and Arvinfar, M. A., "Experimental and Numerical Study of Turbulent Fluid Flow and Heat Transfer of Al2O3/Water Nanofluid in a Spiral-Coil Tube," *Heat Transfer Engineering,* vol. 38, no. 6, pp. 611-626, 2017.

[17] Das, S. K., Putra, N., Thiesen, P., and Roetzel, W., "Temperature dependence of thermal conductivity enhancement for nanofluids," *Journal of Heat Transfer,* vol. 125, no. 4, pp. 567-574, 2003.

[18] Pak, B. C., and Cho, Y. I., "Hydrodynamic and heat transfer study of dispersed fluids with submicron metallic oxide particles," *Experimental Heat Transfer an International Journal,* vol. 11, no. 2, pp. 151-170, 1998.

[19] Corcione, M., "Empirical correlating equations for predicting the effective thermal conductivity and dynamic viscosity of nanofluids," *Energy Conversion and Management,* vol. 52, no. 1, pp. 789-793, 2011.

[20] Kline. S. A., and McClintock, F., "Describing Uncertainties in Single-Sample Experiments," *Mechanical Engineering*, vol. 75, no. 1, pp. 3-8, 1953.

[21] Incropera. F. P., and Dewitt, D. P., Introduction to Heat Transfer, *John WHey & Sons. New York. NY, 1996*.

[22] Gnielinski, V., "New equations for heat and mass transfer in turbulent pipe and channel flow," *International Chemical Engineering,* vol. 16, no. 2, pp. 359-368, 1976.

[23] Huang, D., Wu, Z., and Sunden, B., "Pressure drop and convective heat transfer of Al_2O_3/water and MWCNT/water nanofluids in a chevron plate heat exchanger," *International Journal of Heat and Mass Transfer,* vol. 89, pp. 620-626, 2015.

[24] Vlasogiannis, P., Karagiannis, G., Argyropoulos, P., and Bontozoglou, V., "Air–water two-phase flow and heat transfer in a plate heat exchanger," *International Journal of Multiphase Flow,* vol. 28, no. 5, pp. 757-772, 2002.

[25] Chen, H,. Yang, W., He, Y., Ding, Y,. Zhang, L., Tan, C., *et al.*, "Heat transfer and flow behaviour of aqueous suspensions of titanate nanotubes (nanofluids)," *Powder Technology,* vol. 183, no. 1, pp. 63-72, 2008.

[26] Kumaresan, V., Velraj, R., and Das, S. K., "Convective heat transfer characteristics of secondary refrigerant based CNT nanofluids in a tubular heat exchanger," *International Journal of Refrigeration,* vol. 35, no. 8, pp. 2287-2296, 2012.

[27] Darzi, A. R., Farhadi, M., and Sedighi, K., "Heat transfer and flow characteristics of Al_2O_3–water nanofluid in a double tube heat exchanger," *International Communications in Heat and Mass Transfer,* vol. 47, pp. 105-112, 2013.

[28] Farajollahi, B., Etemad, S. G., and Hojjat, M., "Heat transfer of nanofluids in a shell and tube heat exchanger," *International Journal of Heat and Mass Transfer,* vol. 53, no. 1-3, pp. 12-17, 2010.

[29] Lotfi, R., Rashidi, A. M., and Amrollahi, A., "Experimental study on the heat transfer enhancement of MWNT-water nanofluid in a shell and tube heat exchanger," *International Communications in Heat and Mass Transfer,* vol. 39, no. 1, pp. 108-111, 2012.

[30] Godson, L., Deepak, K., Enoch, C., Jefferson, B., and Raja, B., "Heat transfer characteristics of silver/water nanofluids in a shell and tube heat exchanger," *Archives of Civil and Mechanical Engineering,* vol. 14, no. 3, pp. 489-496, 2014.

[31] Shahrul, I., Mahbubul, I., Saidur, R., Khaleduzzaman, S., Sabri, M., and Rahman, M., "Effectiveness study of a shell and tube heat exchanger operated with nanofluids at different mass flow rates," *Numerical Heat Transfer, Part A: Applications,* vol. 65, no. 7, pp. 699-713, 2014.

[32] Kwon, Y., Kim, D., Li, C., Lee, J., Hong, D., Lee, J., *et al.*, "Heat transfer and pressure drop characteristics of nanofluids in a plate heat exchanger," *Journal of Nanoscience and Nanotechnology,* vol. 11, no. 7, pp. 5769-5774, 2011.

[33] Kabeel, A., El Maaty, T. A., and El Samadony, Y., "The effect of using nano-particles on corrugated plate heat exchanger performance," *Applied Thermal Engineering,* vol. 52, no. 1, pp. 221-229, 2013.

Table 1
The uncertainty results

Accuracy	Heat exchanger type	Reynolds number uncertainty	Maximum uncertainty of heat transfer coefficient
Temperature, ± 0.1 ^{0}C	Double pipe	1%	6%
Mass flow rate, ±1% FS	Shell and tube	1%	4%
Differential pressure transmitter, 0.05% of span	Plate	1%	4%

List of Figure captions

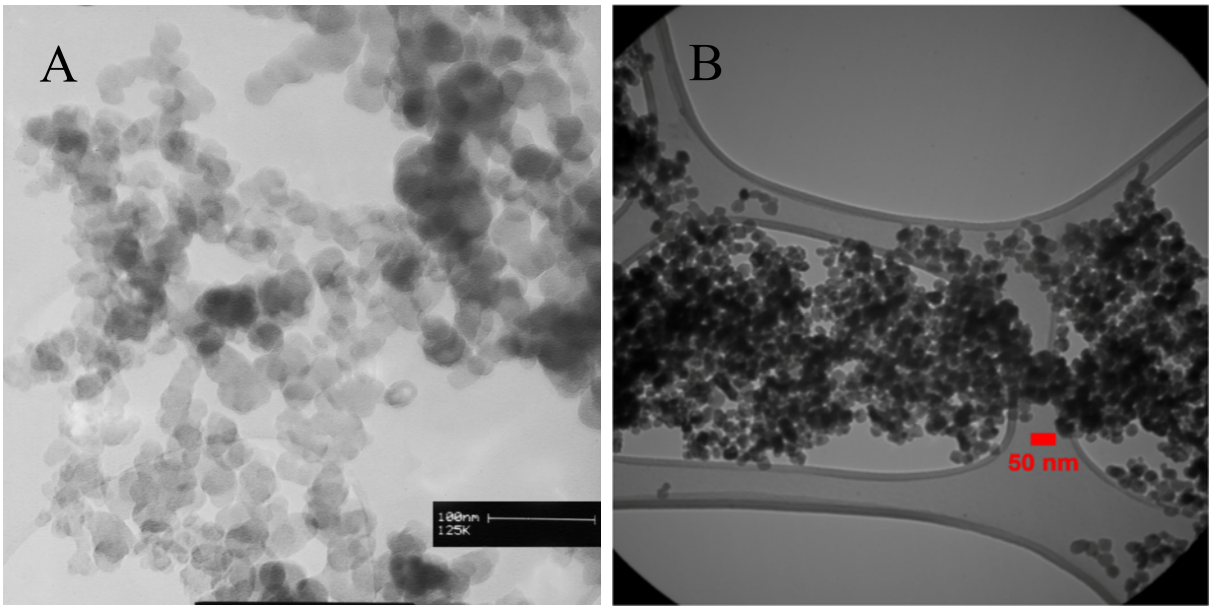

Fig. 1. SEM (A) and TEM (B) images of Al_2O_3 nanoparticles

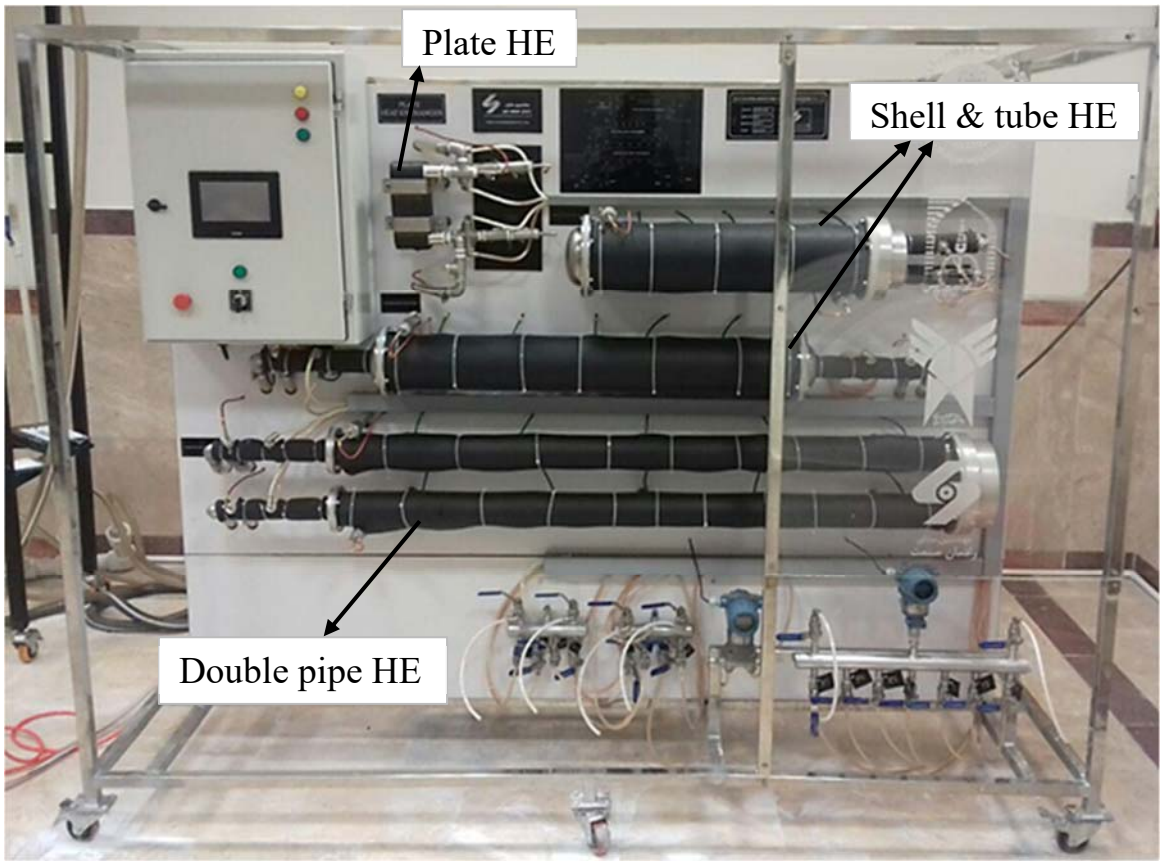

Fig. 2. The experimental setup

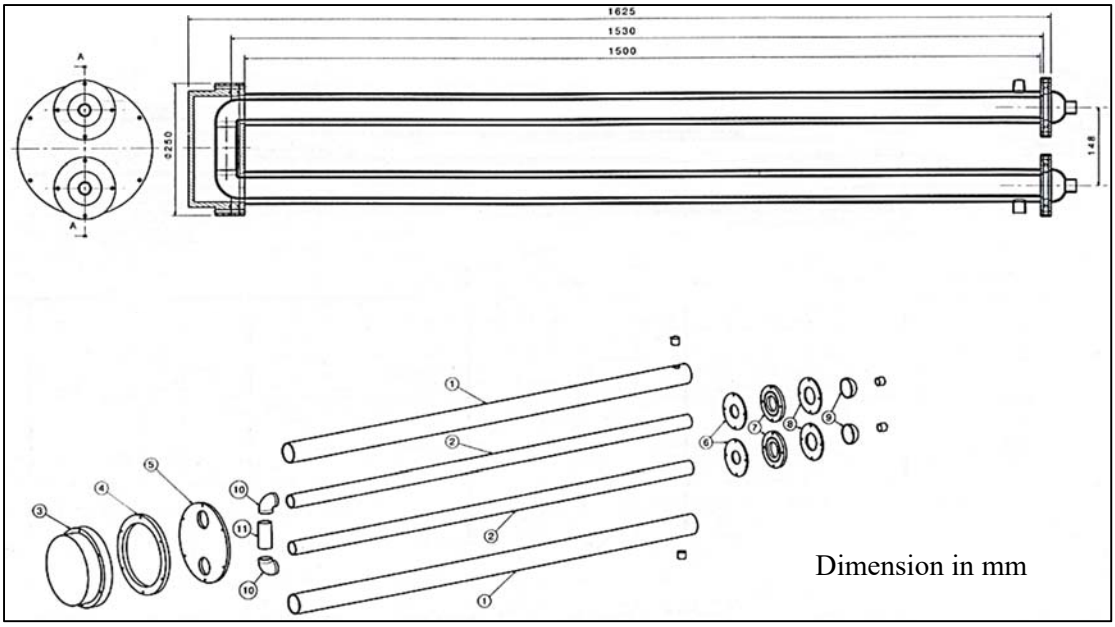

Fig. 3(a). Structure of the double pipe heat exchanger

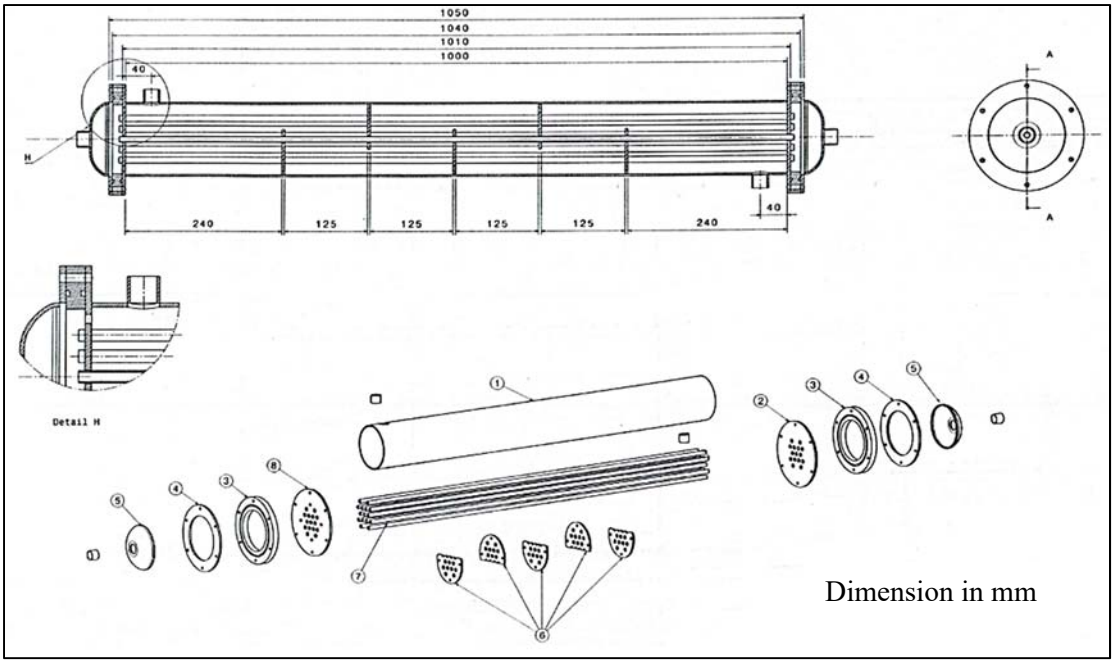

Fig. 3(b). Structure of the shell & tube heat exchanger

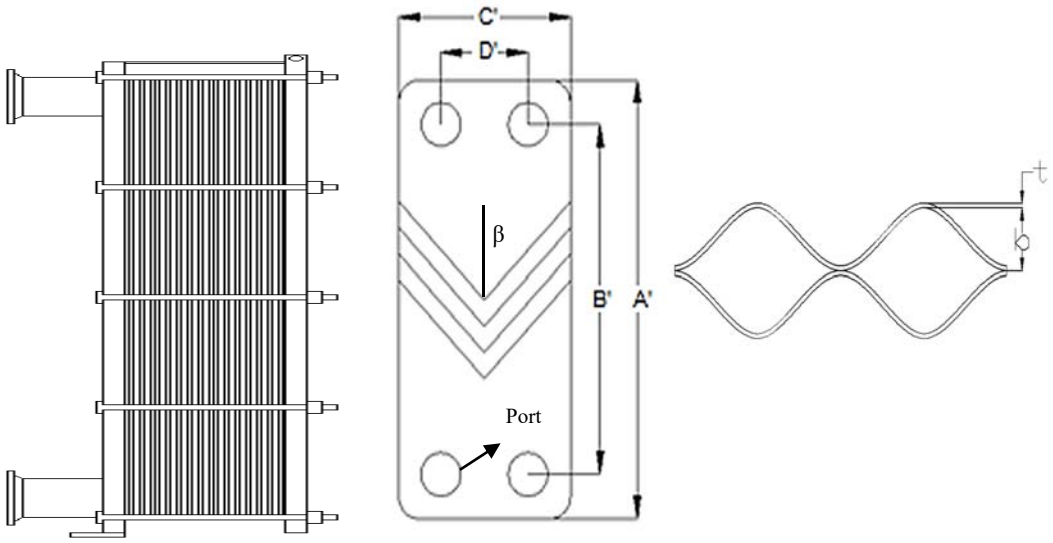

Fig. 3(c). Structure of the plate heat exchanger

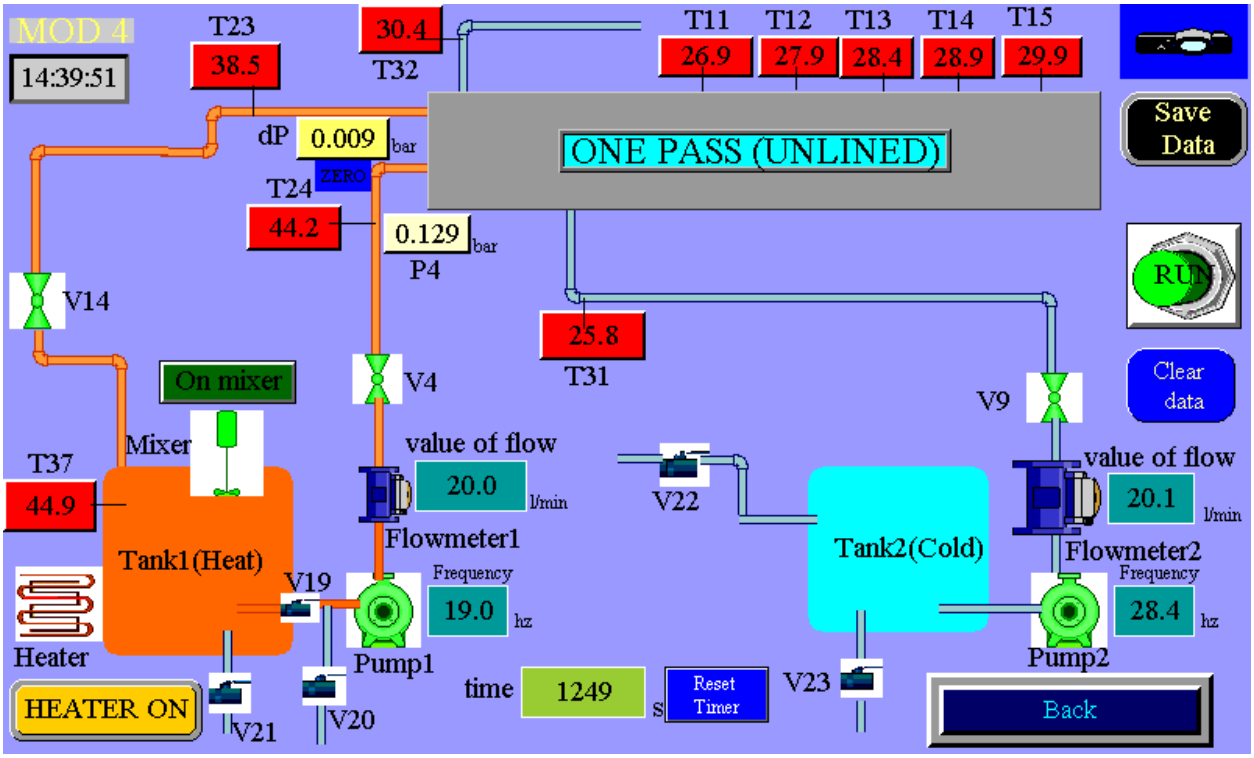

Fig. 4. Monitoring the parameters and results

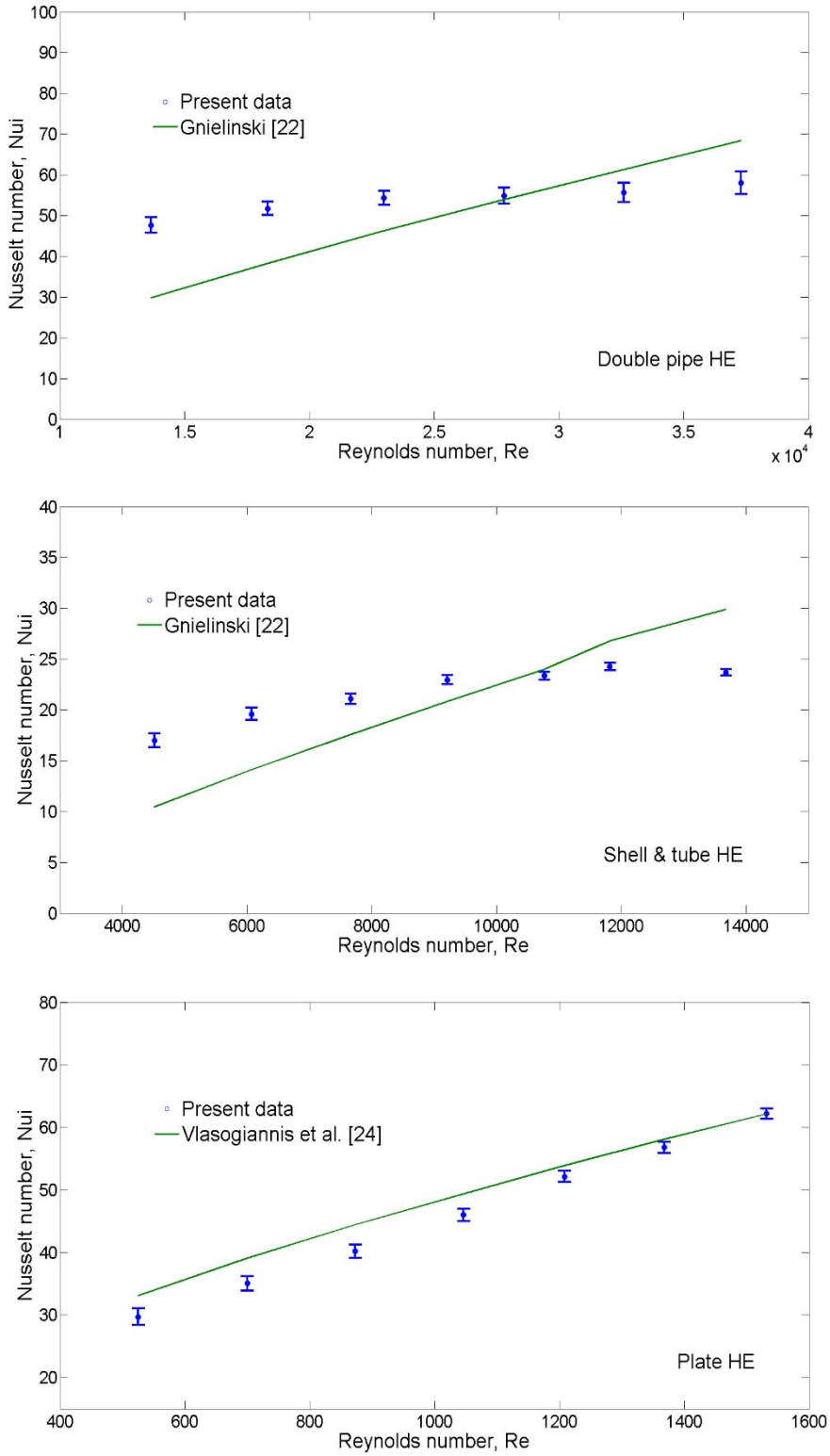

Fig. 5. Comparison of Nu_i with various correlations with respect to Re for different HEs

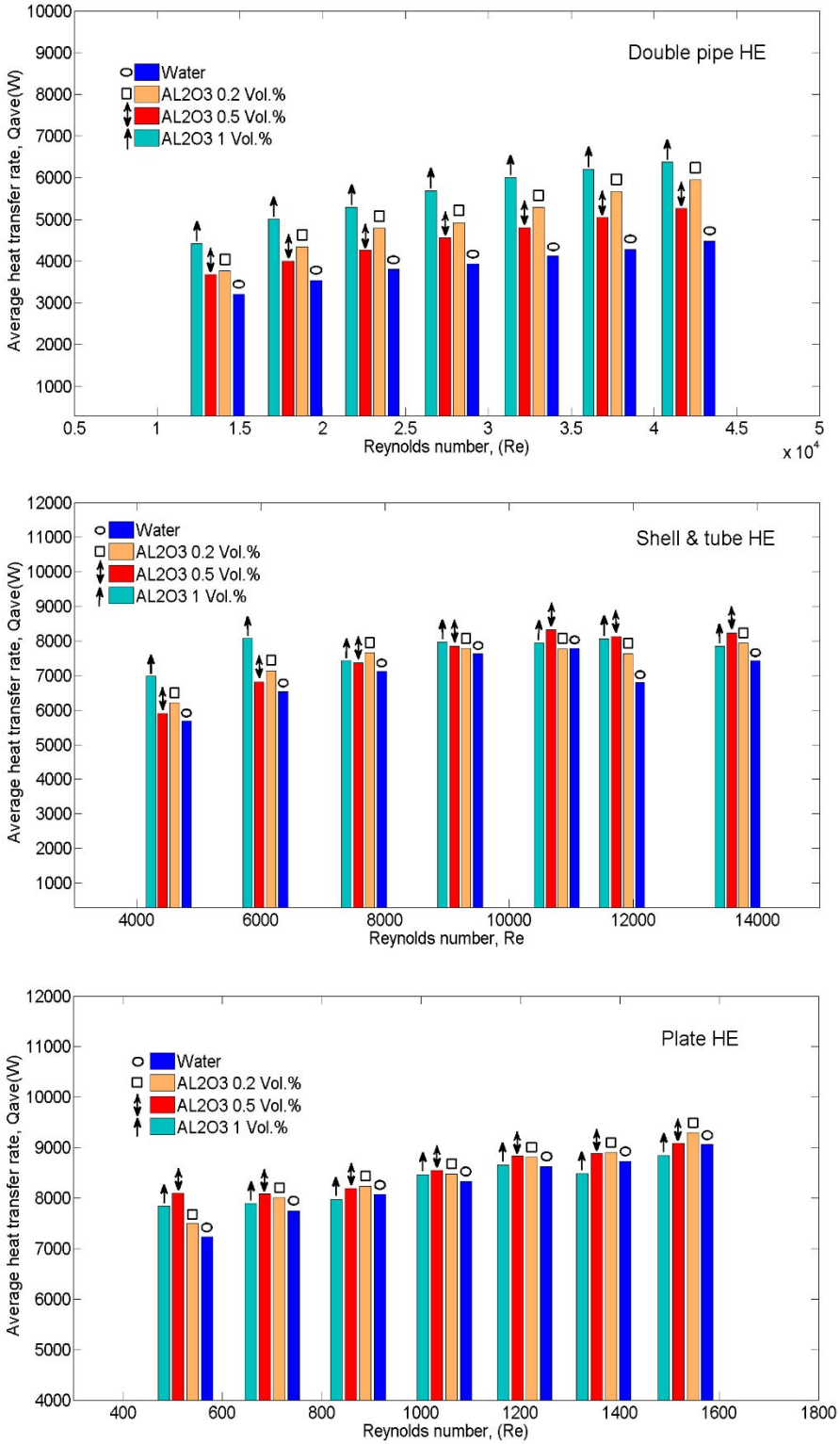

Fig. 6. Variation of Q_{ave} versus *Re* at different nanoparticle concentrations for various HEs

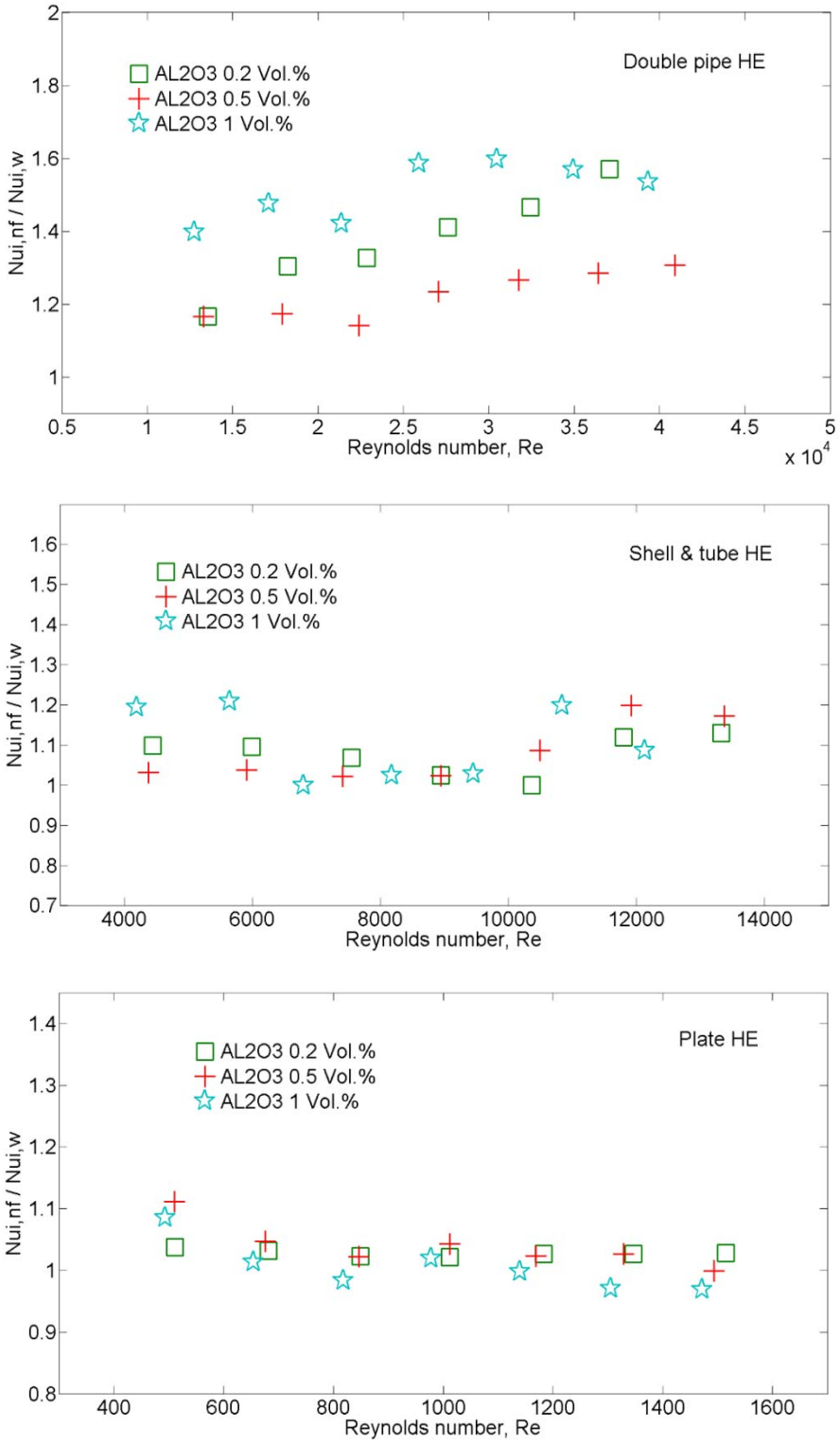

Fig. 7. Variation of Nusselt number ratio versus *Re* at different nanoparticle concentrations for various HEs

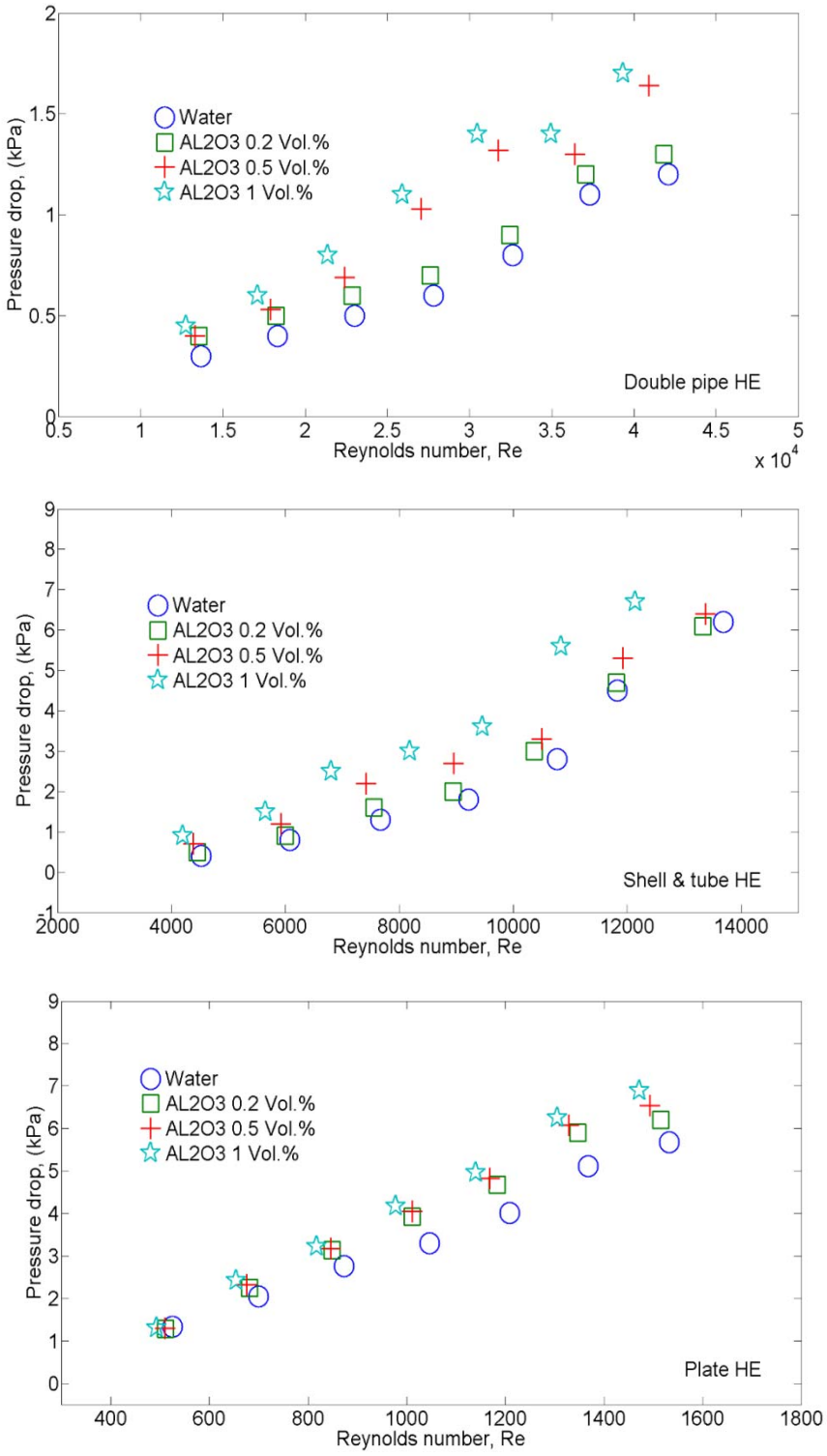

Fig. 8. Variation of ΔP versus *Re* at different nanoparticle concentrations for various HEs

Dariush Mansoury is a faculty member at the Department of Marine Physics, College of Marine Sciences, Tarbiat Modares University, Nour, Iran. He obtained his BSc. and MSc. degrees from the College of Mechanical Engineering, Sharif University of Technology, Tehran, Iran. He also earned his Ph.D. in 2016 in Physical Oceanography at the College of Marine Science & Ocean, Khoramshahr Marine Science and Technology University, Khoramshahr, Iran. His research domain mainly focuses on Simulations (POM), Physical Modeling, and Ocean Dynamics.

Faramarz Ilami Doshmanziari has been working in industries as a technical engineer. He is also active in the Iran Nanotechnology Initiative Council (INIC) as a researcher. He received his M.Sc. degree in energy conversion field from the Department of Mechanical Engineering, Sahand University of Technology, Tabriz, Iran. His research interests include experimental heat transfer, passive and active techniques for heat transfer enhancement, computational fluid dynamics, turbulence modeling, heat exchanger design and optimization. He has authored and co-authored some publications in the related issues.

Abolfazl Kiani is the head of Engineering and Business Development Department at Jam Polypropylene Company in Iran. He received his Ph.D. in Polymer Engineering from Amirkabir University, Tehran, Iran in 2012. His field of study also includes Physical Chemistry of polymers.

Ali J. Chamkha is the Dean of Research, Professor and former Chairman of the Mechanical Engineering Department and Prince Sultan Endowed Chair for Energy and Environment at Prince Mohammad Bin Fahd University (PMU) in the Kingdom of Saudi Arabia. He earned his Ph.D. in Mechanical Engineering from Tennessee Technological University, USA, in 1989. His research interests include multiphase fluid-particle dynamics, nanofluids dynamics, fluid flow in porous media, heat and mass transfer, magnetohydrodynamics and fluid-particle separation. He has served as an Editor, Associate Editor, or a member of the editorial board for many journals such as ASME Journal of Thermal Science and Engineering Applications, International Journal of Numerical Method for Heat and Fluid Flow, Scientia Iranica, Journal of Nanofluids, Recent Patents on Mechanical Engineering, Journal of Applied Fluid Mechanics, International Journal of Fluids and Thermal Sciences, Journal of Heat and Mass Transfer Research, International Journal for Microscale and Nanoscale Thermal and Fluid Transport Phenomena, International Journal of Industrial Mathematics and many others. He has authored and co-authored over 550 publications in archival international journals and conferences.

Mohsen Sharifpur is an Associate Professor in the Department of Mechanical and Aeronautical Engineering at the University of Pretoria and is responsible for the Nanofluids Research Laboratory. He received his B.Sc. (Mechanical Engineering) degree from Shiraz University in Iran. He completed his M.Sc. degree in Nuclear Engineering and received a full scholarship for his Ph.D. study in Mechanical Engineering (Thermal Fluid) from the Eastern Mediterranean University. He is the author and co-author of more than 85 articles and conference papers. His research interests include convective multiphase flow, the thermal fluid behaviour of nanofluids, convective nanofluids, convection in porous media, computational fluid dynamics and waste heat in thermal systems. Professor Sharifpur is rated as a C2 scientist by National Research Foundation (NRF) of South Africa.